



# Model-based analysis of the sensitivities and diagnostic implications of FFR and CFR under various pathological conditions

Xinyang Ge<sup>1,2</sup> | Youjun Liu<sup>3</sup>  | Shengxian Tu<sup>4</sup> | Sergey Simakov<sup>5,6</sup> | Yuri Vassilevski<sup>5,6,7</sup> | Fuyou Liang<sup>1,2,6</sup> 

<sup>1</sup>School of Naval Architecture, Ocean and Civil Engineering, Shanghai Jiao Tong University, Shanghai 200240, China

<sup>2</sup>Collaborative Innovation Center for Advanced Ship and Deep-Sea Exploration (CISSE), Shanghai Jiao Tong University, Shanghai 200240, China

<sup>3</sup>College of Life Science and Bioengineering, Beijing University of Technology, Beijing 100124, China

<sup>4</sup>Med-X Research Institute, School of Biomedical Engineering, Shanghai Jiao Tong University, Shanghai 200030, China

<sup>5</sup>Moscow Institute of Physics and Technology, Dolgoprudny 141700, Russia

<sup>6</sup>Institute for Personalized Medicine, Sechenov University, Moscow 119991, Russia

<sup>7</sup>Institute of Numerical Mathematics, Russian Academy of Sciences, Moscow 119333, Russia

## Correspondence

Fuyou Liang Ph. D, School of Naval Architecture, Ocean and Civil Engineering, Shanghai Jiao Tong University, No. 800 Dongchuan Road, Shanghai 200240, China.  
Email: fuyouliang@sjtu.edu.cn

## Funding information

Russian Foundation for Basic Research, Grant/Award Number: 17-51-53160; SJTU Medical-Engineering Cross-cutting Research Project, Grant/Award Number: YG2016MS09; National Natural Science Foundation of China, Grant/Award Numbers: 11832003 and 81611530715

## Abstract

Although fractional flow reserve (FFR) and coronary flow reserve (CFR) are both frequently used to assess the functional severity of coronary artery stenosis, discordant results of diagnosis between FFR and CFR in some patient cohorts have been reported. In the present study, a computational model was employed to quantify the impacts of various pathophysiological factors on FFR and CFR. In addition, a hyperemic myocardial ischemic index (HMIx) was proposed as a reference for comparing the diagnostic performances of FFR and CFR. Obtained results showed that CFR was more susceptible than FFR to the influence of many pathophysiological factors unrelated to coronary artery stenosis. In particular, the numerical study proved that increasing hyperemic coronary microvascular resistance significantly elevated FFR while reducing CFR despite fixed severity of coronary artery stenosis, whereas introducing aortic valve disease only caused a significant decrease in CFR with little influence on FFR. These results provided theoretical evidence for explaining some clinical observations, such as the increased risk of discordant diagnostic results between FFR and CFR in patients with increased hyperemic microvascular resistance, and significant increase in CFR after surgical relief of severe aortic valve disease. When evaluated with respect to the predictive value for hyperemic myocardial ischemia, the performance of FFR was found to be considerably compromised in the presence of severe coronary vasodilation dysfunction or aortic valve disease, whereas the relationship between CFR and HMIx remained relatively stable, suggesting that CFR may be a more reliable indicator of myocardial ischemia under complex pathophysiological conditions.

## KEYWORDS

aortic valve disease, CFR, FFR, microvascular dilation dysfunction, myocardial ischemia, numerical simulation

## 1 | Introduction

Fractional flow reserve (FFR) and coronary flow reserve (CFR) are widely used hemodynamic indices for evaluating the functional severity of epicardial coronary stenosis.<sup>1,2</sup> Although clinicians prefer to adopt a fixed cut-off value (eg, FFR < 0.8, CFR < 2.0) in FFR- or CFR-based decision making,<sup>3</sup> FFR and CFR can be influenced in different ways or degrees by many factors unrelated to the severity of coronary artery stenosis, such as hyperemic coronary microvascular resistance,<sup>3,4</sup> heart rate<sup>5</sup> and aortic valve disease.<sup>6,7</sup> Another problem often encountered in clinical practice arises from the discordant diagnostic outcomes of FFR and CFR. It has been found that the results of diagnosis with FFR and CFR only agree moderately with each other in the same patient cohort,<sup>3,8</sup> with the distributions of FFR and CFR relative to the cut-off values differing considerably in some patients.<sup>9</sup> Clinical studies have revealed some mechanisms underlying the discordance between FFR and CFR. For instance, FFR-CFR discordance was more likely to be detected in patients with diffuse coronary artery atherosclerosis or small-vessel disease,<sup>10</sup> and increased hyperemic coronary microvascular

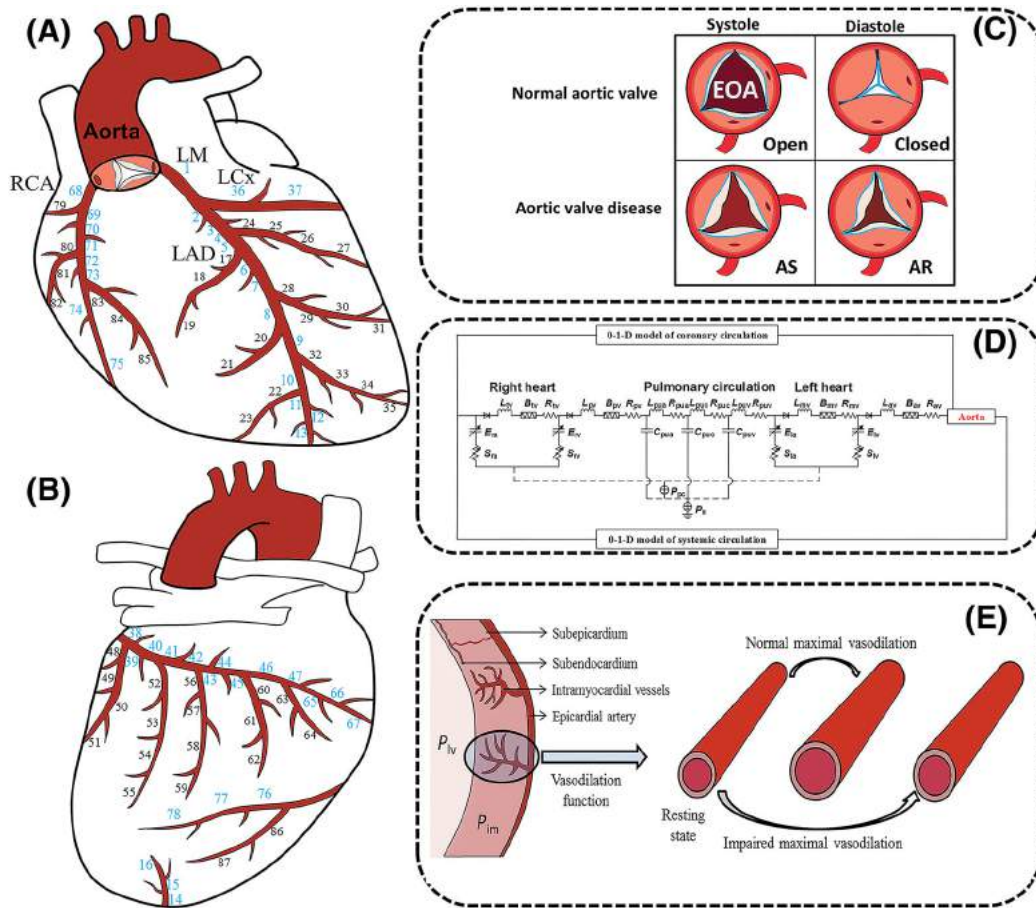


**FIGURE 1** Computational modeling of the coronary circulation coupled with the global cardiovascular system: (A) epicardial coronary arterial tree at the anterior myocardial wall (represented by a 1-D model); (B) epicardial coronary arterial tree at the posterior myocardial wall (represented by a 1-D model); (C) morphology of normal/diseased aortic valve (represented by a lumped parameter model governed by Equations (1) and (2)); (D) configuration of the entire model; (E) diagrammatic descriptions of intramyocardial vessels (represented by a 0-D model) and normal/impaired vasodilation function (adapted from<sup>19</sup> with modifications and represented in the model by adjusting the hyperemic resistance of intramyocardial vessels). Note that (a) penetrating arteries affiliated to the LAD, LCx and RCA trees are numbered as 88-108, 109-129 and 130-140, respectively, which are not shown in panels (A) and (B) in order to simplify the illustration; and (b) detailed descriptions of the 0-1-D model of the systemic circulation and 0-D model of intramyocardial vessels have been reported in,<sup>18,20</sup> respectively. Abbreviations: LM, left main coronary artery; LAD, left anterior descending coronary artery; LCx, left circumflex coronary artery; RCA, right coronary artery; EOA, effective orifice area; AS, aortic valve stenosis; AR, aortic valve regurgitation;  $P_{lv}$ , left ventricular blood pressure;  $P_{im}$ , intramyocardial tissue pressure;  $E$ , elastance;  $L$ , inertance;  $R$ , viscous resistance;  $C$ , compliance;  $B$ , Bernoulli's resistance;  $S$ , viscoelasticity coefficient;  $P_{it}$ , intrathoracic pressure;  $P_{pc}$ , pericardium pressure; ra, right atrium; rv, right ventricle; tv, tricuspid valve; pv, pulmonary valve; pua, pulmonary artery; puc, pulmonary capillary; puv, pulmonary vein; la, left atrium; lv, left ventricle; mv, mitral valve; av, aortic valve

resistance was found to be a major cause of preserved FFR and reduced CFR in patients with intermediate coronary artery stenosis.<sup>3,11,12</sup> Moreover, it was found that patients with a preserved FFR and reduced CFR often experienced higher incidence of cardiac events, whereas patients with a preserved CFR and reduced FFR often had more favorable clinical outcomes,<sup>12</sup> implying the differential prognostic values of FFR and CFR.

Despite the useful insights from existing clinical literature, a systemic investigation on the relationship between FFR and CFR under a wide range of pathophysiological conditions remains absent due to the limitations in *in vivo* measurements and difficulties in isolating the combined effects on FFR and CFR of various pathophysiological factors that differ considerably among patients. In this context, computational models have been utilized as a compensatory tool for quantitatively evaluating the effects on FFR or CFR of various physiological or pathological factors.<sup>13-17</sup> However, none of these studies investigated the sensitivities of FFR and CFR to various pathophysiological factors in a comparative way, nor did they compare the diagnostic values of FFR and CFR.

In the present study, we developed a computational model of the coronary circulation to quantify the respective sensitivities of FFR and CFR to various pathophysiological factors that play important roles in regulating coronary hemodynamics and myocardial perfusion. In particular, we proposed a new index to quantify the degree of functional myocardial ischemia based on the relationship between myocardial energy consumption and coronary blood supply under hyperemic condition, thereby providing a reference for quantitatively comparing the diagnostic performances of FFR and CFR.

## 2 | METHODS

Computational modeling of the coronary circulation has been described in detail in a recent study of our group,<sup>18</sup> where the coronary arterial tree (consisting of 87 large epicardial coronary arteries and 53 penetrating arteries, see Figure 1A,B for a diagrammatic sketch) was represented by a distributed one-dimensional (1-D) model coupled with lumped-parameter (0-D) models of intramyocardial vessels and a 0-1-D model of the cardiovascular system. When a stenosis is present in a coronary artery, the pressure drop across the stenosis was calculated as a function of the trans-stenosis flow rate, and the lumen area and length of the stenosis using a lumped-parameter model.<sup>18</sup> The major geometrical parameters (ie, length, proximal and distal radii of each artery) of the coronary arterial tree and the total baseline resistance and compliance of the intramyocardial vessels (see Figure 1E) distal to each terminal/penetrating coronary artery are listed in Table 1. To enable the model to address the issues of concern in the present study, several modifications were introduced, such as the development of an aortic valve model capable of accounting for the hemodynamic impacts of various valve diseases and a parametric representation of the dilation function of coronary microvasculature.

### 2.1 | Modeling of the aortic valve under normal and pathological conditions

Narrowing of valve orifice area during systole (ie, aortic valve stenosis; AS) and occurrence of flow regurgitation during diastole (ie, aortic valve regurgitation; AR; see Figure 1C) for a diagrammatic description) are common aortic valve abnormalities that not only significantly affect aortic and coronary hemodynamics but also considerably alter the pumping function and energetics of the left ventricle.<sup>21</sup> Although three-dimensional modeling methods can be employed to account for the dynamic motion of valve leaflets and its interaction with blood flow,<sup>22,23</sup> applications of such methods are usually limited to a local aortic valve region due to the high model complexity and computational cost. In contrast, lumped-parameter models of the aortic valve have been widely applied in conjunction with reduced-order models of the global cardiovascular system to address the impacts of valve function on systemic hemodynamics under various pathophysiological conditions.<sup>24,25</sup> In the present study, we modified a lumped-parameter valve model adopted in previous studies<sup>20,26</sup> to enable the representation of trans-valvular hemodynamics under both normal and pathological conditions. In the model, the pressure drop ( $\Delta P$ ) across the aortic valve was related to the trans-valvular flow rate ( $Q_{av}$ ) by

$$\Delta P = R_{av}Q_{av} + B_{av}Q_{av}|Q_{av}| + L_{av}\frac{dQ_{av}}{dt}, \quad (1)$$

where  $R_{av}$ ,  $B_{av}$  and  $L_{av}$  represent the viscous resistance, Bernoullis resistance and blood inertance, respectively, and were taken to be functions of the geometric parameters of the aortic valve and outflow tract.

**TABLE 1** Values of parameters used in the coronary circulation model

No.	$l$	$r_0/r_1$	$R_0$	$C_0$	No.	$l$	$r_0/r_1$	$R_0$	$C_0$
1	12.1	2.40/1.95	-	-	46	23.3	1.00/0.75	-	-
2	3.7	1.92/1.90	-	-	47	18.2	0.75/0.36	-	-
3	7.4	1.90/1.85	-	-	48	18.2	0.36/0.36	-	-
4	7.4	1.85/1.70	-	-	49	10.1	0.88/0.78	-	-
5	3.7	1.70/1.55	-	-	50	18.4	0.78/0.70	-	-
6	6.2	1.55/1.49	-	-	51	14.2	0.70/0.58	3416	$2.1 \times 10^{-4}$
7	6.2	1.49/1.34	-	-	52	14.2	0.58/0.58	-	-
8	6.2	1.34/1.29	-	-	53	6.6	0.70/0.63	-	-
9	15.6	1.29/1.14	-	-	54	14.9	0.63/0.55	-	-
10	7.8	1.14/1.11	-	-	55	10.8	0.55/0.44	3416	$2.1 \times 10^{-4}$
11	12.8	1.11/1.05	-	-	56	10.8	0.44/0.44	-	-
12	25.6	1.05/0.98	-	-	57	6.0	1.47/1.43	-	-
13	22.9	0.98/0.88	-	-	58	12.0	1.43/1.40	-	-
14	15.0	0.88/0.75	-	-	59	9.3	1.40/1.34	3416	$2.1 \times 10^{-4}$
15	7.4	0.75/0.59	-	-	60	4.6	1.34/1.22	-	-
16	3.7	0.59/0.59	2199	$2.1 \times 10^{-4}$	61	6.0	1.22/1.15	-	-
17	7.5	0.98/0.65	-	-	62	12.0	1.15/1.00	3416	$2.1 \times 10^{-4}$
18	14.8	0.65/0.50	-	-	63	12.1	1.00/0.71	-	-
19	11.2	0.50/0.50	2199	$2.1 \times 10^{-4}$	64	6.0	0.71/0.60	3416	$2.1 \times 10^{-4}$
20	6.8	0.55/0.45	-	-	65	12.8	0.6/0.50	-	-
21	10.5	0.45/0.45	2199	$2.1 \times 10^{-4}$	66	34.3	0.50/0.40	-	-
22	6.0	0.55/0.50	-	-	67	21.0	0.40/0.40	3416	$2.1 \times 10^{-4}$
23	11.3	0.50/0.50	2199	$2.1 \times 10^{-4}$	68	6.5	1.30/1.10	-	-
24	10.5	1.05/0.95	-	-	69	15.6	1.10/1.02	-	-
25	21.9	0.95/0.75	-	-	70	3.2	1.02/1.00	-	-
26	16.2	0.75/0.45	-	-	71	17.0	1.00/0.88	-	-
27	16.2	0.45/0.45	2199	$2.1 \times 10^{-4}$	72	27.1	0.65/0.65	-	-
28	10.7	0.95/0.85	-	-	73	25.3	0.80/0.69	-	-
29	20.4	0.85/0.70	-	-	74	30.6	0.69/0.55	-	-
30	15.6	0.70/0.47	-	-	75	9.3	0.55/0.55	-	-
31	15.6	0.47/0.47	2199	$2.1 \times 10^{-4}$	76	39.1	0.75/0.64	-	-
32	8.8	0.85/0.80	-	-	77	30.6	0.64/0.50	-	-
33	17.7	0.80/0.65	-	-	78	10.2	0.50/0.50	1967	$2.1 \times 10^{-4}$
34	13.3	0.65/0.45	-	-	79	24.4	0.48/0.38	1967	$2.1 \times 10^{-4}$
35	13.3	0.45/0.45	2199	$2.1 \times 10^{-4}$	80	24.7	0.38/0.38	-	-
36	8.4	2.15/2.05	-	-	81	19.4	0.88/0.73	-	-
37	5.3	2.05/1.85	-	-	82	36.4	0.73/0.73	1967	$2.1 \times 10^{-4}$
38	9.7	1.85/1.80	-	-	83	16.8	0.60/0.55	-	-
39	5.8	1.80/1.75	-	-	84	18.3	0.55/0.55	-	-
40	3.2	1.75/1.70	-	-	85	18.3	0.98/0.80	1967	$2.1 \times 10^{-4}$
41	3.2	1.70/1.65	-	-	86	30.6	0.80/0.82	-	-

(Continues)

TABLE 1 (Continued)

No.	$l$	$r_0/r_1$	$R_0$	$C_0$	No.	$l$	$r_0/r_1$	$R_0$	$C_0$
42	8.8	1.65/1.60	-	-	87	5.8	0.82/0.82	1967	$2.1 \times 10^{-4}$
43	8.8	1.60/1.45	-	-	88-108	6.0	0.69/0.69	2199	$2.1 \times 10^{-4}$
44	6.5	1.45/1.30	-	-	109-129	6.0	0.69/0.69	3416	$2.1 \times 10^{-4}$
45	13.1	1.20/1.00	-	-	130-140	6.0	0.69/0.69	1967	$2.1 \times 10^{-4}$

Note.  $l$  (mm), length of coronary artery;  $r_0/r_1$  (mm), proximal/distal radius of coronary artery;  $R_0$  (mmHg·s/mL) /  $C_0$  (mL/mmHg), total baseline resistance/compliance of intramyocardial vessels distal to each coronary terminal/penetrating artery.

$$R_{av} = \frac{8\alpha_R\pi\mu l}{(EOA)^2}, B_{av} = \frac{1}{2}\rho\alpha_B\left(\frac{1}{EOA} - \frac{1}{A_{OT}}\right)^2, L_{AV} = 2\pi\rho\alpha_L\sqrt{\frac{1}{EOA} - \frac{1}{A_{OT}}}. \quad (2)$$

Here,  $\mu$  and  $\rho$  represent respectively the dynamic viscosity and density of blood;  $l$  is the effective length of valve leaflet, and  $A_{OT}$  denotes the cross-sectional area of the outflow tract.  $EOA$  represents the effective orifice area of the aortic valve (see Figure 1C). For convenience of notation,  $EOAs$  during diastole and systole were denoted by  $EOA_{dia}$  and  $EOA_{sys}$ , respectively. Accordingly, the values of  $EOA_{dia}$  and  $EOA_{sys}$  could be modulated to account for different types and severities of valve disease. For a normal aortic valve,  $EOA_{sys}$  was set to  $4.0 \text{ cm}^2$  during systole, and  $EOA_{dia}$  was fixed at zero during diastole. In cases of AS,  $EOA_{sys}$  was reduced from  $4.0 \text{ cm}^2$  to  $1.0 \text{ cm}^2$  to represent increasing severity of AS.<sup>27</sup> Similarly,  $EOA_{dia}$  was increased from  $0.0 \text{ cm}^2$  to  $0.3 \text{ cm}^2$  to represent progressive deterioration of AR. As such, the severity of valve disease can be controlled parametrically by adjusting the value of  $EOA$  during systole or diastole. It is noted that due to the insufficiency of Equations (1) and (2) in representing the complex fluid dynamics in the configuration composed by aortic valve leaflets and outflow tract, correction factors  $\alpha_R$  (=0.01),  $\alpha_B$  (=1.0) and  $\alpha_L$  (=1.0) were introduced to calibrate the calculated  $R_{av}$ ,  $B_{av}$  and  $L_{av}$  under the normal valvular condition to those used in previous studies.<sup>20,26,28</sup>

## 2.2 | Modeling of coronary microvascular dilation function

Given the fact that clinical measurements of FFR and CFR both require hyperemic stimulation, the maximal dilation capacity of coronary microvasculature is an important factor affecting the hyperemic response of coronary hemodynamics and the outcome of FFR/CFR measurement. It has been extensively demonstrated that the dilation function of coronary microvasculature can be considerably impaired (see Figure 1E for an illustrative description) in patients with microcirculation dysfunction due to adverse remodeling of coronary arterioles and/or impairment in endothelial function,<sup>19</sup> leading to a blunted resting to hyperemic decrease in microvascular resistance. In the present study, we proposed an index ( $F_{vd}$ ) to quantitatively represent coronary vasodilation function based on the relationship between resting and hyperemic microvascular resistances.

$$F_{vd} = \frac{R_{rs,0} - R_{hp}}{R_{rs,0} - R_{hp,0}} \times 100\%. \quad (3)$$

Here,  $R_{rs,0}$  and  $R_{hp}$  represent microvascular resistances under normal resting condition and hyperemic condition, respectively.  $R_{hp,0}$  represents an ideal state of  $R_{hp}$  and was taken to be  $0.25R_{rs,0}$  based on the clinical observation that the hyperemic resistance of coronary microvasculature reduces to about one fourth of the resting one in patients with normal CFR.<sup>29</sup> It is worth noting that  $R_{hp,0} = 0.25R_{rs,0}$  characterizes a population-averaged rather than subject-specific state of normal vasodilation function given the fact that the relationship between  $R_{hp}$  and  $R_{rs,0}$  has been found to differ considerably among patients with normal CFR.<sup>29</sup> According to Equation (3),  $F_{vd}$  is equal to 100% as  $R_{hp} = R_{hp,0}$  (ie,  $R_{hp}/R_{rs,0} = 0.25$ ), representing the reference normal vasodilation function, and decreases progressively following the increase in the ratio of  $R_{hp}$  to  $R_{rs,0}$ , representing increasing severity of vasodilation dysfunction (see Figure 2). Conversely, given the value of  $F_{vd}$ , the corresponding  $R_{hp}$  can be calculated from Equation (3), and the approach was used to assign  $R_{hp}$  in all the numerical tests that involved  $F_{vd}$  in the present study.

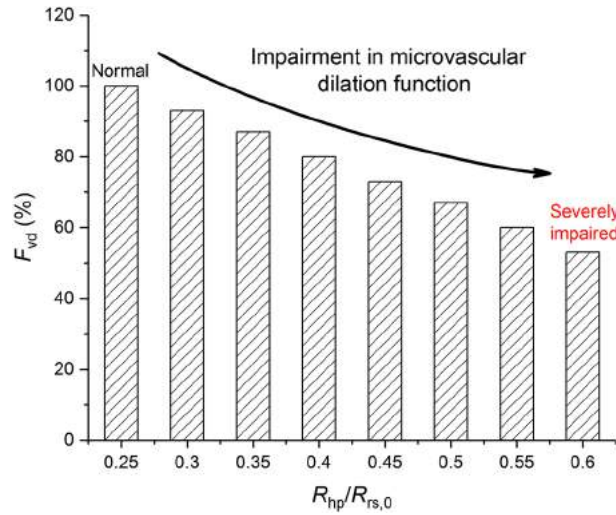


**FIGURE 2** Relationship between coronary vasodilation function index ( $F_{vd}$ ) and the ratio between hyperemic ( $R_{hp}$ ) and resting ( $R_{rs,0}$ ) coronary microvascular resistances

### 2.3 | Parameter assignment

Assignment of model parameters for normal resting and hyperemic conditions was performed in line with the approaches adopted in a previous study,<sup>18</sup> with the assigned major model parameter values being summarized in Table 2. In the case when a stenosis is present in a coronary artery, the resistance of distal coronary microvasculature in resting state was further adjusted to account for the compensatory effect of coronary flow autoregulatory mechanism. Herein, a proportional-integral-derivative (PID) feedback algorithm was applied to iteratively tune the value of microvascular resistance ( $R$ ) so that the model-simulated relationship between perfusion pressure and flow rate matches the flow autoregulation curve (plotted in Figure 3) established based on experimental data. The PID feedback algorithm was expressed in discrete form, with  $R$  and flow rate ( $Q$ ) being the target variable and driving variable, respectively.

$$R^{k+1} = R^k \left[ K_p cor(k) + K_i \sum_{j=0}^k cor(j) + K_d (cor(k) - cor(k-1)) \right], \quad (4)$$

with  $cor(k) = 1 + \frac{Q^k - Q^R}{Q^R}$ .

Here,  $R^k$  and  $R^{k+1}$  represent the microvascular resistances at the  $k$ th and the  $(k+1)$ th iteration steps, respectively.  $K_p$ ,  $K_i$  and  $K_d$  represent the proportional term, integral term and differential term, respectively.  $Cor(k)$  is a correction function established based on the model-simulated mean flow rate ( $Q^k$ ) and the target mean flow rate ( $Q^R$ ) on the

**TABLE 2** Values of major parameters in the coronary and systemic models assigned for normal resting and hyperemic conditions

Parameter	Resting state	Hyperemic state
$C_{cor}$ (mL/mmHg)	0.011	0.011
$E_{Iva}$ (mmHg/mL)	2.87	3.44
HR (beats/min)	67	96
$R_{LAD}$ (mmHg·s/mL)	78.53	20.54
$R_{LCx}$ (mmHg·s/mL)	126.53	38.34
$R_{RCA}$ (mmHg·s/mL)	122.91	33.92
$R_{sys}$ (mmHg·s/mL)	1.14	0.98

*Note.*  $C_{cor}$ , total baseline compliance of intramyocardial vessels;  $E_{Iva}$ , peak systolic elastance of the left ventricle; HR, heart rate;  $R_{LAD}/R_{LCx}/R_{RCA}$ , total baseline resistance of intramyocardial vessels distal to LAD/LCx/RCA;  $R_{sys}$ , total vascular resistance of the systemic circulation. It is noted that  $C_{cor}$  in hyperemic condition was set to be the same with that in resting condition due to the lack of reference data from available literature.

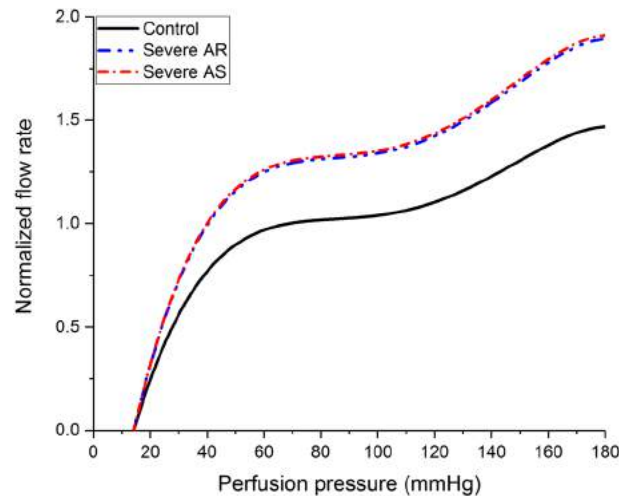


**FIGURE 3** Coronary flow autoregulation curves represented in form of the relationships between coronary perfusion pressure and normalized (by the reference flow rate computed under normal resting condition) mean flow rate under control condition and in the presence of severe aortic valve disease (ie, aortic valve regurgitation [AR] or aortic valve stenosis [AS]). In the presence of severe AR or AS, the normalized flow rate has been shifted upward in proportion to the degree of increase in left ventricular *PVA* relative to that in the control condition

autoregulation curve. In the present study, convergence of the iterative computation was judged when  $|cor(k)-1| < 0.005$ . More details on the parameter tuning method have been described elsewhere.<sup>18</sup>

In the presence of aortic valve disease, further parameter adjustments are required because the deteriorated hemodynamic conditions will increase left ventricular workload and myocardial oxygen demand,<sup>21,30,31</sup> ultimately inducing adaptive remodeling of both myocardium and coronary vascular bed in order to regulate myocardial stress and maintain the balance between myocardial oxygen consumption (demand) and coronary oxygen delivery (supply).<sup>21,32,33</sup> Moreover, systemic hemodynamics may also be altered by aortic valve disease and modulated by compensatory mechanisms. Clinical studies showed that mean aortic blood pressure in patients with severe AR was about 10 mmHg/4 mmHg lower than in control subjects under resting/hyperemic condition<sup>21</sup> but was nearly preserved in patients with severe AS.<sup>34</sup> In the present study, we elevated the systemic vascular resistance in proportion to the severity of aortic valve disease to partly recover aortic blood pressure. Under resting/hyperemic condition, the model-simulated aortic pressure was 80.84 mmHg/87.07 mmHg and 90.0 mmHg/85.03 mmHg in the presence of severe AR and AS, respectively, and their differences with the control values (95.45 mmHg/88.39 mmHg) were basically comparable with the clinical data. With regard to coronary blood flow in the presence of aortic valve disease, we assumed that the amount of blood supply to the myocardium under resting condition was proportional to myocardial oxygen consumption estimated by the pressure-volume area (*PVA*) of the left ventricle. Accordingly, resting coronary blood flow rate was adjusted via modifying coronary microvascular resistance with the method described by Equation (4) but with the flow autoregulation curve being up-adjusted based on the ratio between the *PVA* computed for the aortic valve disease condition and the reference *PVA* under the control condition (see Figure 3). Under hyperemic condition, we assumed that the resistance of coronary microvasculature was the same as that in the control condition. Our numerical results showed that the computed total hyperemic coronary blood flow was 13.79 mL/s and 13.02 mL/s in the presence of severe AR and AS, respectively; both were close to the value (14.26 mL/s) under the control condition, which was consistent with the clinical observation that the maximal coronary blood flow rates in patients with aortic valve disease did not differ significantly from those in the control cohort.<sup>35</sup> Table 3 shows the model-simulated mean aortic blood pressure and blood flow rate in a coronary artery (artery No. 27 in Figure 1A) with various severities of stenosis under resting/hyperemic condition in the absence or presence of severe aortic valve disease.

## 2.4 | Definitions of FFR, CFR, and hyperemic myocardial ischemic index

FFR is a blood pressure-based index, defined as the ratio between the mean blood pressure distal to a coronary artery stenosis and the mean blood pressure in the ascending aorta under hyperemic condition [1]; whereas CFR is a blood

**TABLE 3** Computed mean aortic blood pressure, blood flow rate, post-stenosis pressure (ie, distal pressure), fractional flow reserve (FFR) and coronary flow reserve (CFR) in a coronary artery (artery No. 27 in Figure 1A in the absence (ie,  $SR = 0\%$ ) of or with a stenosis of various severities ( $SR = 50\%$ ,  $60\%$  and  $70\%$ ) under control and several representative pathological conditions

Stenosis rate	Control/pathological condition	Resting state		Hyperemic state			FFR	CFR
		Aortic pressure (mmHg)	Flow rate (mL/s)	Aortic pressure (mmHg)	Distal pressure (mmHg)	Flow rate (mL/s)		
$SR = 0\%$	Normal	95.45	0.0209	88.39	82.78	0.0860	0.937	4.115
	Severe CMD	95.45	0.0209	95.34	93.07	0.0370	0.976	1.770
	Severe AS	90.00	0.0263	85.03	79.97	0.0756	0.941	2.875
	Severe AR	80.84	0.0259	87.07	81.63	0.0805	0.938	3.108
$SR = 50\%$	Control	95.45	0.0208	88.40	76.92	0.0707	0.870	3.398
	Severe CMD	95.45	0.0208	95.34	90.42	0.0330	0.948	1.587
	Severe AS	89.99	0.0263	85.04	74.62	0.0640	0.878	2.434
	Severe AR	80.84	0.0259	87.07	75.98	0.0682	0.873	2.633
$SR = 60\%$	Control	95.45	0.0208	88.41	71.22	0.0573	0.806	2.755
	Severe CMD	95.45	0.0208	95.35	87.18	0.0306	0.914	1.471
	Severe AS	90.00	0.0262	85.04	69.40	0.0527	0.816	2.012
	Severe AR	80.84	0.0257	87.08	70.49	0.0561	0.810	2.183
$SR = 70\%$	Control	95.45	0.0208	88.42	61.04	0.0367	0.690	1.748
	Severe CMD	95.45	0.0208	95.35	78.73	0.0244	0.826	1.173
	Severe AS	90.00	0.0260	85.06	60.08	0.0333	0.706	1.281
	Severe AR	80.84	0.0253	87.09	60.57	0.0357	0.695	1.411

*Note.* The control condition means that neither coronary microvascular dilation dysfunction (CMD) nor aortic valve disease is present. Note that, in order to save space, post-stenosis pressure in resting state is not provided because it is not used in the calculation of fractional flow reserve (FFR) or coronary flow reserve (CFR).

flow-based index, defined as the ratio of hyperemic to resting mean flow rate in a coronary artery of interest.<sup>2</sup> Figure 4 shows the model-simulated blood pressure/flow waveforms under resting and hyperemic conditions and the corresponding FFR and CFR in a branch (ie, artery No. 27 in Figure 1A) of the left anterior descending coronary artery (LAD) free of stenosis or in the presence of a 70% stenosis. As expected, introducing a 70% stenosis in the coronary artery significantly reduced post-stenosis blood pressure and hyperemic blood flow, causing a marked decrease in both FFR and CFR.

As mentioned previously, although both FFR and CFR can be used to assess the impact of coronary artery stenosis on myocardial perfusion, they have been found to give discordant diagnostic results in some patients. In this study, we defined a new index, namely hyperemic myocardial ischemic index (HMIx), based on the pressure-volume area (PVA) of the left ventricle and coronary arterial flow rate under hyperemic condition to provide a reference for comparing the performances of FFR and CFR in predicting the severity of impaired myocardial perfusion.

$$\text{HMIx} = 1 - \frac{Q_{\text{hp}}}{PVA_{\text{hp}}} / \frac{Q_{\text{hp},0}}{PVA_{\text{hp},0}} \quad (5)$$

Herein,  $Q_{\text{hp},0}$  and  $PVA_{\text{hp},0}$  represent respectively the reference values of the hyperemic blood flow rate in a coronary artery of interest and left ventricular PVA under normal condition (ie, in the absence of coronary artery stenosis, aortic valve disease and coronary microcirculation dysfunction), with their counterparts under various pathological conditions being denoted by  $Q_{\text{hp}}$  and  $PVA_{\text{hp}}$ , respectively. Left ventricular PVA is the total area circumscribed by the end-systolic pressure-volume (PV) line, the end-diastolic PV curve and the systolic PV trajectory and is often taken to be a measure of the total workload of the left ventricle.<sup>36-38</sup> Because it has been demonstrated that PVA always correlates linearly with myocardial oxygen consumption under various pathophysiological conditions,<sup>36,37</sup> PVA can be used to estimate the demand of myocardial oxygen supply. Given that oxygen supply to the heart muscle is proportional to the amount of coronary blood flow,<sup>33,39,40</sup> the ratio of  $Q_{\text{hp}}$  to  $PVA_{\text{hp}}$  can be taken as a measure of the balance between coronary blood supply and myocardial perfusion demand. Assuming that  $Q_{\text{hp},0}/PVA_{\text{hp},0}$  represents the optimal state, HMIx will increase from 0 toward a maximal value of 1 following the decrease in coronary blood flow or increase in PVA, reflecting different degrees of myocardial ischemia. To test the sensitivity of HMIx to changes in coronary blood flow and/or PVA, we



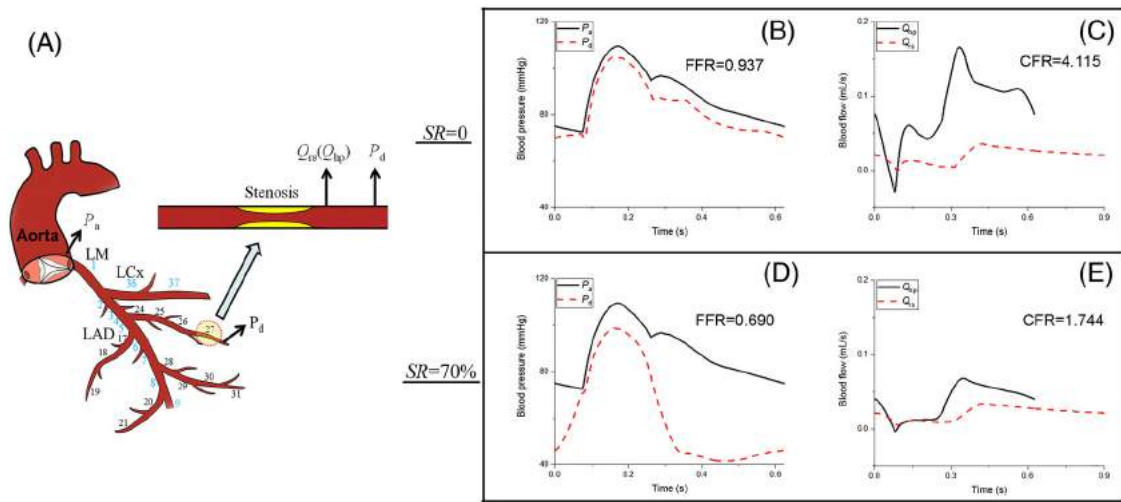


**FIGURE 4** (A) Diagram of the location of stenosis and the places where hemodynamic data used for computing fractional flow reserve (FFR) and coronary flow reserve (CFR) are monitored, and model-simulated blood (B and D) pressure/(C and E) flow waveforms in the ascending aorta and/or in a coronary artery free of stenosis (indicated by  $SR = 0\%$ ) or with a 70% stenosis under resting condition and hyperemic condition, respectively. The computed FFR or CFR is given in each corresponding panel. Notations:  $P_a$  and  $P_d$  are blood pressures in the aorta and the post-stenosis region of the coronary artery, respectively; and  $Q_{rs}$  and  $Q_{hp}$  represent the resting and hyperemic blood flow rates in the coronary artery, respectively

performed numerical simulations under normal hyperemic condition and various pathological conditions characterized by the presence of a 70% stenosis in a LAD branch (ie, artery No. 27 in Figure 1A) combined with severe coronary vasodilation dysfunction ( $F_{vd} = 53\%$ ) or severe AS ( $EOA_{sys} = 1.0 \text{ cm}^2$ ). Figure 5 shows the model-simulated left ventricular PV loops, PVAs and blood flow waveforms in the coronary artery. HMIx was, as expected, equal to 0 in normal hyperemic condition and increased to 0.56 following the introduction of the coronary artery stenosis, which significantly reduced the amount of blood supplied to the left ventricular myocardium. Introducing severe coronary vasodilation dysfunction further reduced hyperemic coronary arterial flow and introducing AS significantly increased PVA, causing HMIx to increase from 0.56 to 0.74 and 0.71, respectively. The numerical tests indicate that HMIx can properly reflect the severity of myocardial ischemia induced by reduced coronary blood flow, increased cardiac workload or a combination of them. In this sense, HMIx can be utilized as a reference for evaluating the predicative values of FFR and CFR for myocardial ischemia in cases where quantitative in vivo measurement of myocardial ischemia is not available. On the other hand, it should be noted that the use of blood flow rate in a local coronary artery in the calculation of HMIx

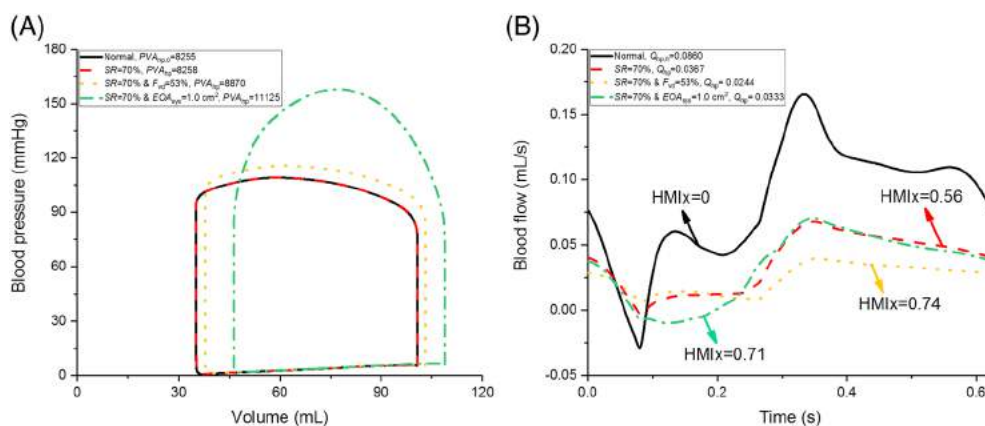


**FIGURE 5** (A) Simulated pressure-volume loops of the left ventricle and (B) blood flow waveforms in a left anterior descending coronary artery (LAD) branch (artery No. 27 in Figure 1A) under normal hyperemic condition and various pathological conditions. Hyperemic myocardial ischemic index (HMIx) is calculated for each case based on the left ventricular pressure-volume area (PVA, mmHg·mL) and mean coronary blood flow rate ( $Q$ , mL/s), with the result being plotted jointly with the corresponding flow waveform.  $SR$  (stenosis rate) = 70% denotes the presence of a severe stenosis in the coronary artery, and  $F_{vd} = 53\%$  and  $EOA_{sys} = 1.0 \text{ cm}^2$  represent the pathological conditions characterized by severely impaired coronary microvascular dilation function and severe aortic valve stenosis, respectively

determines that HMIx can only reflect the ischemic severity of the local myocardial district supplied by the coronary artery rather than of the global myocardium.

## 2.5 | Numerical experiments

Numerical experiments were first carried out to investigate the respective sensitivities of FFR and CFR to variations in various cardiovascular parameters expected to considerably affect coronary hemodynamics under hyperemic condition. Subsequently, numerical simulations were performed with the incorporation of various degrees of coronary vasodilation dysfunction and aortic valve disease to address their impacts on FFR and CFR and the associated diagnostic performances. As common computation conditions, heart rate was fixed at 67 beats/min for resting condition and 96 beats/min for hyperemic condition, and stenotic conditions were introduced to a branch (ie, artery No. 27 in Figure 1 A) of the LAD, with the length of stenosis being fixed at 5 mm despite variations in stenosis severity (quantified by diameter stenosis rate). Accordingly, FFR and CFR were computed and presented only for artery No. 27 unless stated otherwise.

## 3 | RESULTS

### 3.1 | Influences of aortic valve disease on systemic and coronary hemodynamics

Numerical simulations were run under normal resting condition and two pathological conditions characterized respectively by the presence of severe AR (ie,  $EOA_{dia} = 0.3 \text{ cm}^2$ ) and severe AS (ie,  $EOA_{sys} = 1.0 \text{ cm}^2$ ). Figure 6 shows that AR leads to pronounced widening of the aortic pulse pressure, whereas AS causes a marked augmentation of the pressure gradient between the left ventricle and aorta. These changes were accompanied by remarkable alterations of the left ventricular (PV) loop and the flow velocity waveform in the proximal segment of the LAD (see Figure 7). For instance, AR led to an increase in stroke volume, and AS caused the systolic portion of the P-V loop to shift upward. With regard to the flow velocity waveform in the LAD, the waveform simulated for the severe AR condition was featured by an augmented systolic component. In contrast, a marked decrease of coronary flow velocity in systole was observed in the case of AS. These model-simulated features of coronary arterial flow waveform are basically consistent with previous clinical observations.<sup>41,42</sup> Quantitatively, the simulated systolic to diastolic coronary flow velocity-time integral was 0.33 under the normal condition and increased to 0.46 in the presence of severe AR, both were comparable with the reported in vivo data (0.32 vs. 0.65<sup>42</sup>). In the presence of severe AS, the simulated systolic to diastolic velocity-time integral decreased to 0.25, agreeing well with the measured data (0.26).<sup>42</sup>

### 3.2 | Sensitivities of FFR and CFR to variations in cardiovascular parameters

Sensitivity analyses were performed under three coronary artery stenosis conditions (ie, the diameter stenosis rate of a stenosis in a LAD branch [ie, artery No. 27 in Figure 1A] was set to 50%, 60% and 70%, respectively). The selected cardiovascular parameters are those involved in the regulation of coronary hemodynamics under hyperemic condition, including the total coronary microvascular compliance ( $C_{cor}$ ), systolic elastance of the left ventricle ( $E_{lva}$ ), heart rate ( $HR$ ), total coronary microvascular resistance ( $R_{cor}$ ) and total systemic vascular resistance ( $R_{sys}$ ). The reference values of these parameters have been reported in Table 2. Note that  $R_{cor}$  is a holistic description of  $R_{LAD}$ ,  $R_{LCx}$ , and  $R_{RCA}$  in Table 2, and its variation was implemented through varying the three resistances simultaneously. Each set of parameter sensitivity analysis was performed by varying the value of each selected parameter by  $\pm 25\%$  relative to its reference

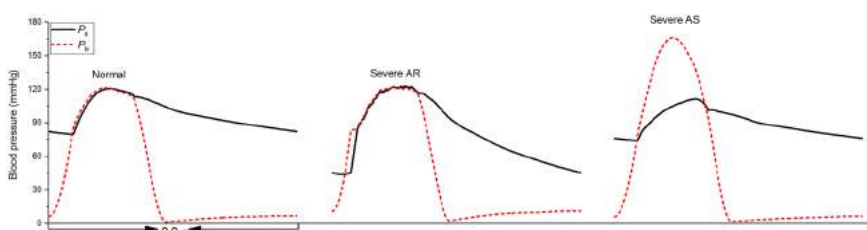


**FIGURE 6** Simulated blood pressure waveforms in the left ventricle ( $P_{IV}$ ) and the aorta ( $P_a$ ) under normal resting condition and pathological conditions characterized by the presence of severe aortic valve regurgitation (AR) or aortic valve stenosis (AS)

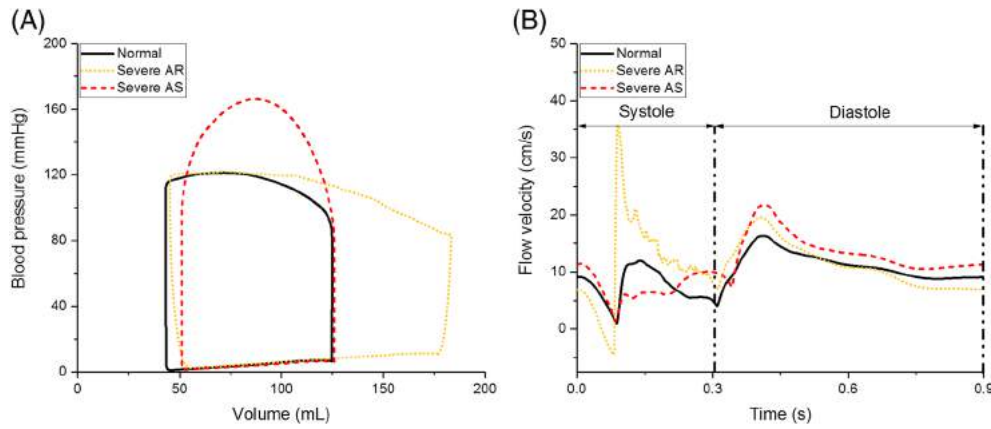


**FIGURE 7** Simulated pressure-volume loops of the left ventricle and flow velocity waveforms in the proximal portion of the left anterior descending coronary artery (LAD) under normal resting condition and pathological conditions characterized by the presence of severe aortic valve regurgitation (AR) or aortic valve stenosis (AS)

value while keeping other parameters at their reference states. To facilitate quantitative comparison, the percentage changes (relative to the simulated FFR and CFR at the reference state) in computed FFR and CFR upon the variation in each parameter were calculated and plotted in Figure 8, with the absolute values of FFR and CFR being reported in Table 4. In comparison with FFR, CFR was sensitive (judged by a relative percentage change in FFR/CFR of >5%) to more parameters and exhibited larger changes in response to parameter variations. For instance, FFR was sensitive solely to  $R_{cor}$ , whereas CFR was sensitive not only to  $R_{cor}$  but also to  $R_{sys}$  and  $HR$ . In another word,  $R_{cor}$  was the only common parameter to which FFR and CFR are sensitive, and its influence on FFR and CFR will be investigated more extensively in the following section through varying  $F_{vd}$  (related closely to  $R_{cor}$  under hyperemic condition [ie,  $R_{hp}$ ] according to Equation (3)). The effects of variations in other parameters (eg,  $R_{sys}$  and  $HR$ ) to which FFR is insensitive will not be addressed in further detail.

### 3.3 | Influences of coronary vasodilation dysfunction and aortic valve disease on FFR and CFR

Various degrees of coronary vasodilation dysfunction were introduced to the model by means of incrementally increasing the ratio between hyperemic resistance ( $R_{hp}$ ) and resting (baseline) resistance ( $R_{rs,0}$ ) of coronary microvasculature from the reference value (ie,  $R_{hp}/R_{rs,0} = 0.25$ ) to 0.6 (which corresponded with a decrease of  $F_{vd}$  from 100% [normal vasodilation function] to 53% [severely impaired vasodilation function] according to Equation 3; see Figure 2). The severities of AR and AS were controlled by the values assigned to  $EOA_{dia}$  and  $EOA_{sys}$  in Equation (2), respectively. Accordingly, the coexistence of AR and AS of various severities was represented by assigning different values to  $EOA_{dia}$

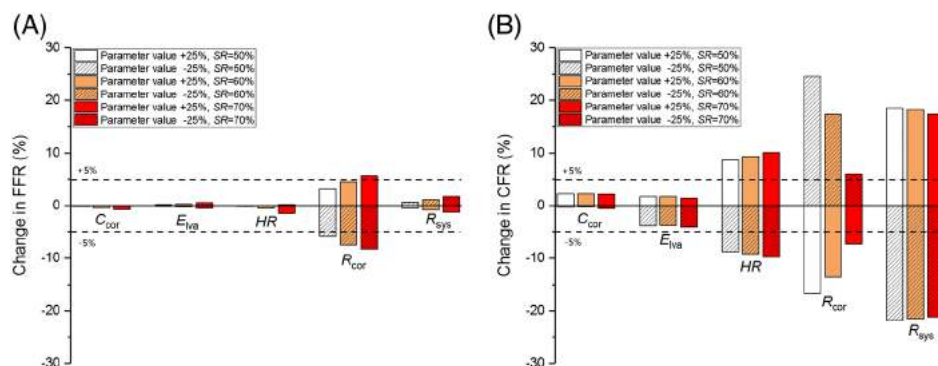


**FIGURE 8** Changes (in percentage) in simulated (A) fractional flow reserve (FFR) and (B) coronary flow reserve (CFR) upon  $\pm 25\%$  variations in each individual cardiovascular parameter relative to its reference value under three coronary artery stenosis conditions (ie, SR [stenosis rate] is set to 50%, 60% and 70%, respectively)

**TABLE 4** Computed fractional flow reserve (FFR) and coronary flow reserve (CFR) in parameter sensitivity analysis

Reference	FFR			CFR		
	SR = 50% (0.870)	SR = 60% (0.806)	SR = 70% (0.690)	SR = 50% (3.398)	SR = 60% (2.755)	SR = 70% (1.748)
$R_{\text{sys}}$ (+25%)	0.866	0.799	0.682	4.028	3.258	2.052
$R_{\text{sys}}$ (-25%)	0.876	0.815	0.703	2.658	2.163	1.378
$R_{\text{cor}}$ (+25%)	0.898	0.842	0.729	2.831	2.381	1.620
$R_{\text{cor}}$ (-25%)	0.820	0.745	0.634	4.235	3.234	1.853
HR (+25%)	0.869	0.802	0.680	3.692	3.011	1.924
HR (-25%)	0.870	0.806	0.692	3.100	2.504	1.577
$E_{\text{lva}}$ (+25%)	0.872	0.808	0.694	3.456	2.803	1.772
$E_{\text{lva}}$ (-25%)	0.869	0.804	0.687	3.269	2.651	1.677
$C_{\text{cor}}$ (+25%)	0.869	0.803	0.685	3.475	2.817	1.786
$C_{\text{cor}}$ (-25%)	0.870	0.806	0.691	3.389	2.751	1.739

Note. In each set of sensitivity analysis, we introduced a stenosis of various severities (indicated by SR) in a left anterior descending coronary artery (LAD) branch (No. 27 in Figure 1A) and varied the value of a selected model parameter by  $\pm 25\%$  relative to its reference value while keeping other parameters unchanged. The reference values of fractional flow reserve (FFR)/coronary flow reserve (CFR) were computed by keeping all model parameters involved the sensitivity analysis at their reference states. Note that all the parameter values are those assigned for hyperemic condition and  $R_{\text{cor}}$  represents the total baseline resistance of all intramyocardial vessels, whose variation is implemented by simultaneously varying  $R_{\text{LAD}}$ ,  $R_{\text{LCx}}$  and  $R_{\text{RCA}}$  in Table 2 in the same degree.

and  $EOA_{\text{sys}}$ . These conditions were combined with various coronary artery stenosis conditions represented by varying the diameter stenosis rate (SR) of a stenosis introduced in a LAD branch (artery No. 27 in Figure 1A) from 0% (no stenosis) to 75% (severe stenosis).

Figure 9 plots the computed FFR/CFR with respect to coronary artery stenosis rate under various vasodilation dysfunction conditions. Each curve represents the results obtained for a fixed  $F_{\text{vd}}$  while varying stenosis rate. It is evident that, given fixed severity of coronary artery stenosis, increasing the severity of vasodilation dysfunction (ie, reducing  $F_{\text{vd}}$ ) led to a marked increase in FFR and a decrease in CFR. The influence of vasodilation dysfunction on FFR was more pronounced in the presence of moderate to severe coronary artery stenosis; whereas CFR was more evidently affected by vasodilation dysfunction when the severity of coronary artery stenosis was mild to moderate. With regard to the influences of aortic valve disease on FFR and CFR, Figure 10 shows that increasing the severity of AR and/or AS, similar to the impairment of coronary vasodilation function, tends to increase FFR while reducing CFR. However, the magnitudes of changes in FFR were much smaller than those of CFR, indicating that aortic valve disease only significantly affects CFR.

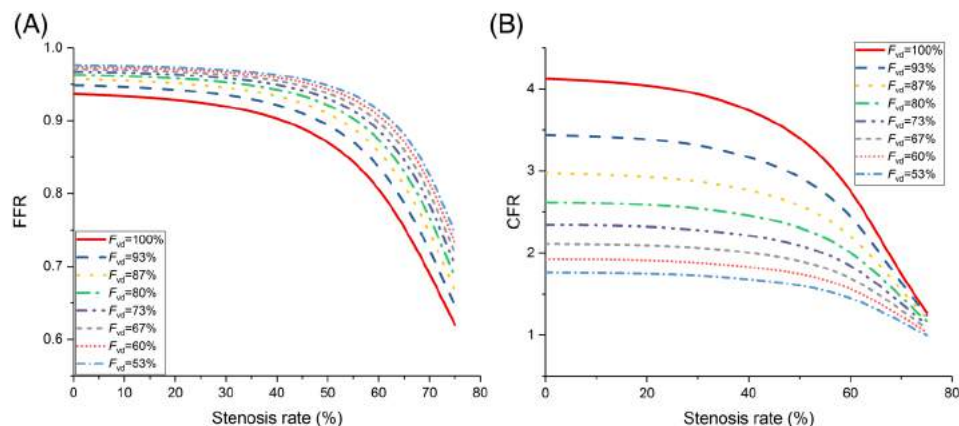


**FIGURE 9** Influences of coronary microvascular dilation dysfunction (with its severity being quantitatively represented by the value of  $F_{\text{vd}}$ ) on (A) fractional flow reserve (FFR) and (B) coronary flow reserve (CFR) under different coronary artery stenosis conditions (represented by varying the stenosis rate from 0% to 75%)

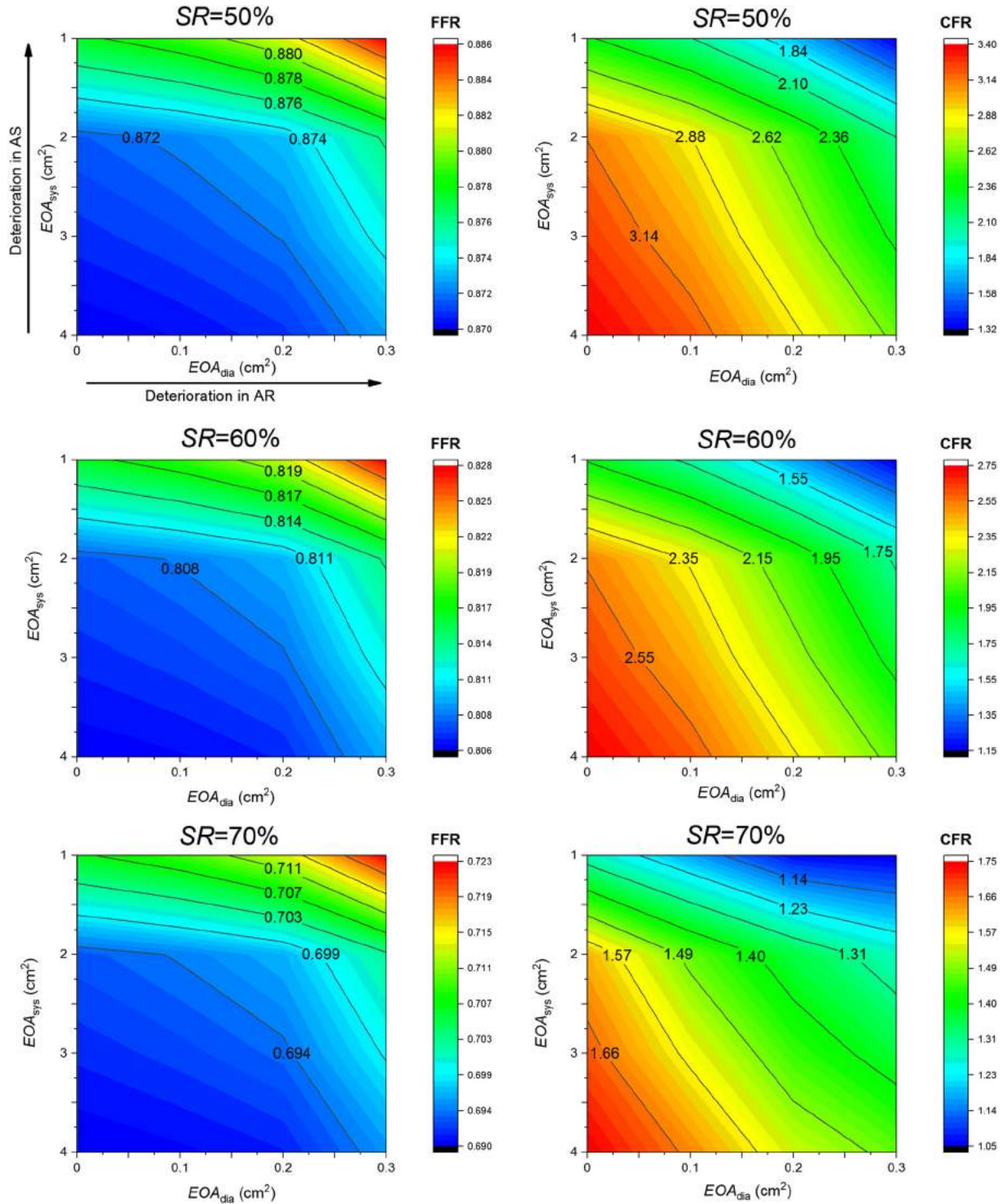


**FIGURE 10** Contour plots of computed fractional flow reserve (FFR) and coronary flow reserve (CFR) under three coronary artery stenosis conditions (ie, SR is set to 50%, 60% and 70%, respectively) combined with various aortic valve disease conditions. The severities of aortic valve regurgitation (AR) and aortic valve stenosis (AS) are represented by the values of  $EOA_{dia}$  and  $EOA_{sys}$ , respectively; please see the text following Equation (2) for more details

### 3.4 | HMIx-based evaluation of the diagnostic performances of FFR and CFR

Figure 11 plots the model-simulated HMIx under the pathological conditions described in Section 3.3 with respect to the corresponding FFR and CFR, respectively. Each line labeled with a value of  $F_{vd}$  or  $EOA$  represents the HMIx-FFR/CFR

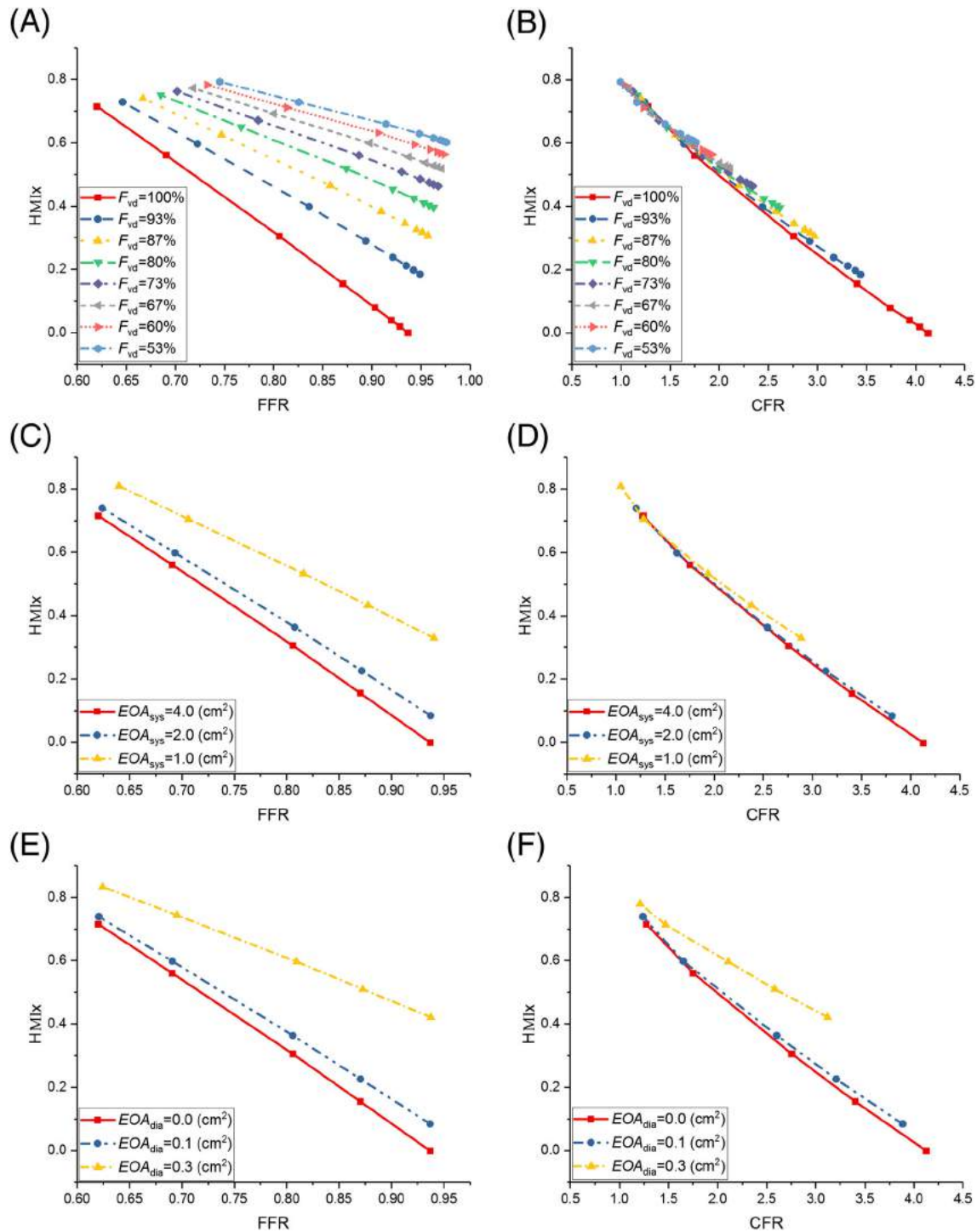


**FIGURE 11** Relationships between HMIx and FFR/CFR under various pathological conditions characterized by the coexistence of coronary artery disease with coronary vasodilation dysfunction or aortic valve disease

relationship obtained for a fixed state of vasodilation dysfunction or aortic valve disease while varying severity of coronary artery stenosis (ie,  $SR$  is varied from 75% to 0%). Panels (A), (C) and (E) show that the value of HMIx corresponding to each FFR value is not constant but changes over a wide range depending on the status of coronary vasodilation function or the severity of aortic valve disease. Specifically, given a fixed FFR value, the value of HMIx increased with the deterioration of both coronary vasodilation dysfunction and aortic valve disease, indicating that the performance of FFR as an indicator of myocardial ischemia is significantly compromised in the presence of vasodilation dysfunction or aortic

valve disease. In contrast, the relationship between HMIx and CFR was only mildly influenced by coronary vasodilation dysfunction and aortic valve disease (see panels (B), (D) and (F)).

## 4 | DISCUSSION

In the present study, a computational model of the coronary circulation was employed to simulate FFR and CFR under various pathophysiological conditions. Main contributions of the study lie in two aspects: (a) investigated the sensitivities of FFR and CFR to various pathophysiological factors in a comparative way; and (b) compared the diagnostic implications of FFR and CFR based on a proposed hyperemic myocardial ischemic index.

Clinical studies have demonstrated that CFR is more sensitive to coronary hemodynamic states affected by not only local coronary lesions but also the functional statuses of coronary microvasculature and systemic circulation,<sup>43</sup> whereas FFR is better correlated with the severity of epicardial coronary lesion.<sup>8,44</sup> These observations are well supported by our numerical results that CFR was significantly affected by a variety of pathophysiological factors unrelated to the severity of coronary artery stenosis, including hyperemic coronary microvascular resistance, heart rate and systemic vascular resistance as well as aortic valve disease, whereas FFR was sensitive solely to the hyperemic resistance of coronary microcirculation. The model-based finding of hyperemic coronary microvascular resistance as a common sensitive factor for FFR and CFR is consistent with the clinical observation that hyperemic coronary microvascular resistance or its determinant factors (eg, myocardial capillary density) had significant influence on both FFR and CFR.<sup>3,4,45,46</sup> In particular, our numerical study revealed that depressing the vasodilation function of coronary microcirculation (which is represented by reducing  $F_{vd}$  and incorporated in the model by increasing hyperemic coronary microvascular resistance) had opposite influence on FFR and CFR, making FFR and CFR behave oppositely when crossing the cut-off lines (ie,  $FFR = 0.8$ ,  $CFR = 2.0$ ) due to the influence of vasodilation dysfunction in the presence of moderate to critical coronary artery stenosis (see Figure 9), which can explain why discordant diagnostic results with FFR and CFR were more frequently encountered in patients with intermediate coronary artery stenosis and high hyperemic microvascular resistance.<sup>3,11</sup> In addition, the model-based finding regarding the mild influence of aortic valve disease on FFR and marked influence on CFR can account for the insignificant change in FFR before and after the treatment of AS,<sup>7</sup> the much lower CFR in patients with AS or AR in comparison with the controls<sup>6,21</sup> and the significant increase in CFR after interventional relief of aortic valve disease.<sup>6</sup> Overall, the differential sensitivities and responses of FFR and CFR to coronary stenosis-independent factors play an important role in modulating the relationship between FFR and CFR and represent an important mechanism underlying the discordant diagnostic results of FFR and CFR in patients with comparable severity of coronary artery disease and different cardiovascular conditions.

Although CFR is more susceptible than FFR to the influences from many pathophysiological factors unrelated to coronary artery stenosis, the comparison of FFR and CFR, with respect to the predictive value for myocardial ischemia under hyperemic condition (herein quantified by HMIx), revealed an opposite phenomenon. From the results presented in Figure 11, the predictive value of FFR for HMIx was considerably compromised by both coronary vasodilation dysfunction and aortic valve disease, whereas the relationship between CFR and HMIx remained relatively stable despite the introduction of various pathological conditions. For instance, when FFR was equal to 0.8 (the frequently adopted cut-off value of FFR in clinical decision making), HMIx was 0.32 in the control condition but increased to 0.75 and 0.61 respectively following the introduction of severe coronary vasodilation dysfunction (ie,  $F_{vd} = 53\%$ ) and severe aortic regurgitation (ie,  $EOA_{dia} = 0.3 \text{ cm}^2$ ). That is to say, the same FFR value does not always indicate the same severity of myocardial ischemia. In addition, from the slope of each HMIx-FFR line (generated by fixing the severity of vasodilation dysfunction or aortic valve disease while varying the severity of coronary artery stenosis), the degree of improvement in hyperemic myocardial perfusion (herein assessed by the reduction in HMIx) brought by removing a severe coronary artery stenosis indicated by a FFR of  $<0.8$  was significantly attenuated in the presence of severe vasodilation dysfunction compared with the case of normal vasodilation function. The discrepancy in myocardial ischemia prediction between FFR and CFR is largely determined by the difference in hemodynamic quantities from which they are derived. Given fixed severity of coronary artery stenosis, post-stenosis blood pressure, as a major determinant of FFR, is inversely related to trans-stenosis blood flow rate. In the presence of coronary vasodilation dysfunction, the increased hyperemic resistance of coronary microcirculation reduces hyperemic blood flow to deteriorate myocardial ischemia but increases FFR by elevating post-stenosis blood pressure, leading the change in FFR to exhibit a positive rather than clinically expected negative relation with the severity of myocardial ischemia. In contrast, CFR, calculated as the ratio between hyperemic blood flow rate and resting (baseline) blood flow rate, decreases with the vasodilation dysfunction-induced reduction in hyperemic blood flow and

hence can better reflect the status of hyperemic myocardial perfusion. In the presence of aortic valve disease, although hyperemic blood flow usually remains comparable with that in the control condition,<sup>35</sup> resting coronary blood flow is increased to match increased cardiac workload through compensatory alterations of coronary microvasculature. The differential influences of aortic valve disease on resting and hyperemic blood flows determine that FFR (calculated based on blood pressures under hyperemic condition) is less affected, whereas CFR is considerably reduced due to the compensatory increase in resting blood flow and preserved hyperemic blood flow (see Figure 10). As a consequence, CFR is more sensitive than FFR to the augmented imbalance between blood supply and increased cardiac workload caused by aortic valve disease under hyperemic condition.

The model-based findings regarding the complicated relationships among FFR, CFR and HMIx under various pathological conditions may be utilized to explain some clinical observations or guide decision making. Coexistence of coronary artery disease with coronary microvascular dysfunction and/or aortic valve disease is not uncommon. It has been found that coronary microvascular dysfunction, which is featured mainly by impaired vasodilation function and increased hyperemic microvascular resistance, has a prevalence of 51%-54% in patients with suspected coronary artery disease.<sup>19</sup> Aortic valve disease of moderate to severe degree was detected in 8.5% to 13% of the population,<sup>47</sup> and among patients with severe aortic valve disease, the prevalence of coronary artery disease was in the range of 40% to 75%.<sup>7</sup> The study by van de Hoef et al.<sup>4</sup> revealed that the prevalence of inducible myocardial ischemia (detected with myocardial perfusion scintigraphy) was significantly higher in patients with high hyperemic microvascular resistance than in those with low hyperemic microvascular resistance despite equivalent FFR. Similarly, it was found that poor prognosis was associated closely with increased hyperemic microvascular resistance in patients with preserved FFR and low CFR.<sup>11,48</sup> These clinical findings can be explained by the model-predicted increase/decrease in FFR/CFR with the increase in hyperemic coronary microvascular resistance and the impaired predictive value of FFR and preserved predictive value of CFR for HMIx. For the case of concomitant coronary artery disease and aortic valve disease, although clinical studies dedicated to comparing the prognostic values of FFR and CFR are rare, it can be speculated from our numerical results that CFR may be a more reliable indicator of myocardial ischemia in patients with this kind of pathological condition. Therefore, special caution should be taken when interpreting FFR and CFR measured in patients suffering from concomitant coronary artery disease and coronary microvascular dysfunction or aortic valve disease. A negative diagnosis with FFR does not always mean that hyperemic myocardial ischemia is at a tolerable level, whereas a positive diagnosis with CFR does not always indicate the presence of a severe coronary artery stenosis. For these patients, if the severity of myocardial ischemia were the main evidence for decision making, CFR, which has been found to exhibit a stable coherence to HMIx over a wide range of pathophysiological conditions, may be a more reliable indicator than FFR.

## 5 | LIMITATIONS

This study has several limitations. First, the model-predicted critical diameter stenosis rate (*SR*) for  $FFR < 0.8$  under the control condition was about 60%, which is slightly larger than the stenosis rates ( $53.5\% \pm 10.7\%$ ) of coronary artery lesions with  $FFR \leq 0.8$  reported in a clinical study.<sup>49</sup> In another clinical study, using a *SR* of  $\geq 50\%$  for predicting  $FFR \leq 0.8$  was found to have a statistically significant accuracy of 0.64, although  $FFR > 0.8$  was present in a considerable portion of patients with  $SR \geq 50\%$ .<sup>50</sup> The discrepancy between our numerical prediction and clinical observations might have been caused by the simplified modeling of stenosis in our study where only the stenosis length and stenosis rate were incorporated, which rendered the model unable to account for intra-stenosis flow disturbances induced by the complex stenosis morphology under in vivo conditions, thereby leading to underestimation of the trans-stenosis pressure gradient and accordingly a relatively higher prediction of FFR (eg,  $FFR = 0.87$  when  $SR = 50\%$ ). The speculation is supported by the clinical finding that coronary artery lesions with complex geometries had reduced FFRs compared with lesions without complex geometries.<sup>50</sup> This limitation would not alter our finding regarding the differential sensitivities of FFR and CFR to various pathological factors but may deserve consideration and need further improvement if the model is applied to predict patient-specific FFR. Second, our numerical results have been obtained by varying a limited number of selected model parameters while fixing other parameters at the reference state. In reality, cardiovascular conditions may differ considerably among patients and would exert complex influences on FFR and CFR beyond those presented in the study. In this sense, the findings of our study would contribute rather as a theoretical reference for interpreting some population-averaged clinical observations than as a criterion for judging the clinical significance of FFR and CFR measured in individual patients. Third, our numerical tests have been performed on a LAD branch,



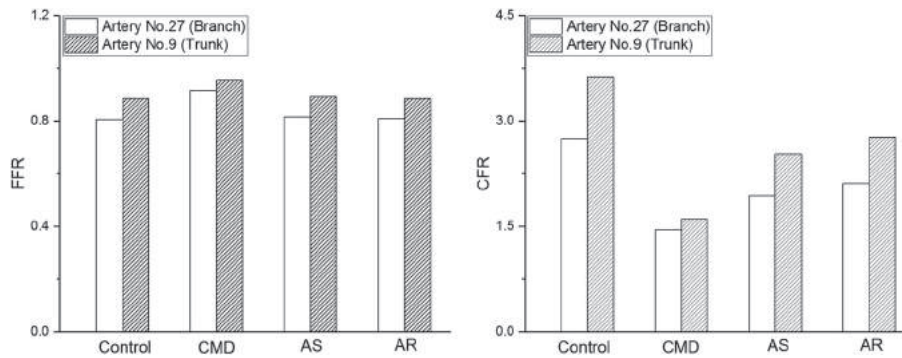


**FIGURE 12** Comparisons of model-simulated fractional flow reserve (FFR)/coronary flow reserve (CFR) in a 60% stenosed left anterior descending coronary artery (LAD) trunk (artery No. 9 in Figure 1A) versus a 60% stenosed LAD branch (artery No. 27 in Figure 1A) under control and various pathological conditions (ie, coronary microvascular dilation dysfunction [CMD] or aortic valve disease). CMD, aortic valve stenosis (AS) and aortic valve regurgitation (AR) are all at a severe state as quantitatively represented by  $F_{vd} = 53\%$ ,  $EOA_{sys} = 1.0 \text{ cm}^2$  and  $EOA_{dia} = 0.3 \text{ cm}^2$ , respectively

although clinically significant stenotic lesions are more commonly detected in large coronary arteries. Theoretically, our methods can be applied to investigate the sensitivities of FFR and CFR in all the coronary arteries included in the model. We chose a branch artery as the object of study mainly in consideration of computational cost rather than due to technical limitations. In comparison with stenosis present in a branch artery, a severe stenosis present in a large coronary artery will significantly alter hemodynamics in a wider territory of downstream coronary vessels and require longer computational time to tune vascular resistances (defined by Equation (4)) based on the flow autoregulation mechanism. To confirm that our methods are applicable to large coronary arteries as well, we performed additional numerical tests on a LAD trunk (artery No. 9 in Figure 1A) with a 60% stenosis. The results showed that the responses of FFR/CFR to the introduction of vasodilation dysfunction or aortic valve disease did not differ qualitatively from those found for the LAD branch (artery No. 27 in Figure 1A), although the computed FFR/CFR values differed considerably between the trunk and branch due to the differential local hemodynamic conditions in these arteries (see Figure 12). Finally, although hyperemic myocardial ischemic index (HMIx) has been defined based on well-established physiological knowledge and is expected to provide an indirect measure of the imbalance between coronary blood supply and myocardial energetic demand, it is by far a proposed index in the absence of sufficient clinical validation. Further clinical studies would be needed to confirm the validity of HMIx as an indicator of myocardial ischemia as well as determine the clinically significant threshold value.

## 6 | CONCLUSIONS

Model-based numerical experiments have been performed to comparatively investigate the sensitivities and diagnostic implications of FFR and CFR under various pathophysiological conditions. CFR was proved to be more sensitive than FFR to various pathophysiological factors unrelated to coronary artery stenosis. In particular, the model-based finding regarding the opposite influence of coronary vasodilation dysfunction on FFR and CFR provided theoretical evidence for explaining the clinically observed high risk of discordant diagnostic results between FFR and CFR in patients with intermediate coronary artery disease and increased hyperemic coronary microvascular resistance. Moreover, the predictive value of FFR for myocardial ischemia evaluated by the proposed HMIx was found to be significantly compromised in the presence of severe coronary vasodilation dysfunction or aortic valve disease, whereas the relationship between CFR and HMIx remained relatively stable, which suggests that CFR may be a more reliable indicator of myocardial ischemia under complex pathophysiological conditions.

## ACKNOWLEDGEMENT

The study was supported by the National Natural Science Foundation of China (Grant no. 11832003, 81611530715) and the SJTU Medical-Engineering Cross-cutting Research Project (Grant no. YG2016MS09). Sergey Simakov and Yuri Vassilevski were supported by the Russian Foundation for Basic Research (Grant no. 17-51-53160).

## CONFLICT OF INTEREST STATEMENT

The authors have no conflicts of interest to declare.

## ORCID

Youjun Liu  <https://orcid.org/0000-0003-4251-1071>

Fuyou Liang  <https://orcid.org/0000-0001-5012-486X>

## REFERENCES

1. Pijls NH, De Bruyne B, Peels K, et al. Measurement of fractional flow reserve to assess the functional severity of coronary-artery stenoses. *N Engl J Med*. 1996;334(26):1703-1708.
2. Gould KL, Kirkeeide RL, Buchi M. Coronary flow reserve as a physiologic measure of stenosis severity. *J Am Coll Cardiol*. 1990;15(2):459-474.
3. Meuwissen M, Chamuleau SA, Siebes M, et al. Role of variability in microvascular resistance on fractional flow reserve and coronary blood flow velocity reserve in intermediate coronary lesions. *Circulation*. 2001;103(2):184-187.
4. van de Hoef TP, Nolte F, Echavarría-Pinto M, et al. Impact of hyperaemic microvascular resistance on fractional flow reserve measurements in patients with stable coronary artery disease: Insights from combined stenosis and microvascular resistance assessment. *Heart*. 2014;100(12):951-959.
5. Rossen JD, Winniford MD. Effect of increases in heart rate and arterial pressure on coronary flow reserve in humans. *J Am Coll Cardiol*. 1993;21(2):343-348.
6. Wiegerinck EM, van de Hoef TP, Rolandi MC, et al. Impact of aortic valve stenosis on coronary hemodynamics and the instantaneous effect of transcatheter aortic valve implantation. *Circ Cardiovasc Interv*. 2015;8(8):e002443.
7. Pesarini G, Scarsini R, Zivelonghi C, et al. Functional assessment of coronary artery disease in patients undergoing transcatheter aortic valve implantation: Influence of pressure overload on the evaluation of lesions severity. *Circ Cardiovasc Interv*. 2016;9(11):e004088.
8. Meimoun P, Sayah S, Luyckx-Bore A, et al. Comparison between non-invasive coronary flow reserve and fractional flow reserve to assess the functional significance of left anterior descending artery stenosis of intermediate severity. *J Am Soc Echocardiogr*. 2011;24(4):374-381.
9. van de Hoef TP, Echavarría-Pinto M, van Lavieren MA, et al. Diagnostic and prognostic implications of coronary flow capacity: A comprehensive cross-modality physiological concept in ischemic heart disease. *JACC Cardiovasc Interv*. 2015;8(13):1670-1680.
10. Johnson NP, Kirkeeide RL, Gould KL. Is discordance of coronary flow reserve and fractional flow reserve due to methodology or clinically relevant coronary pathophysiology? *JACC Cardiovasc Imaging*. 2012;5(2):193-202.
11. Lee JM, Jung J-H, Hwang D, et al. Coronary flow reserve and microcirculatory resistance in patients with intermediate coronary stenosis. *J Am Coll Cardiol*. 2016;67(10):1158-1169.
12. Ahn SG, Suh J, Hung OY, et al. Discordance between fractional flow reserve and coronary flow reserve: Insights from intracoronary imaging and physiological assessment. *JACC Cardiovasc Interv*. 2017;10(10):999-1007.
13. Siebes M, Chamuleau SA, Meuwissen M, et al. Influence of hemodynamic conditions on fractional flow reserve: Parametric analysis of underlying model. *Am J Physiol Heart Circ Physiol*. 2002;283(4):H1462-H1470.
14. Huo Y, Svendsen M, Choy JS, Zhang ZD, Kassab GS. A validated predictive model of coronary fractional flow reserve. *J R Soc Interface*. 2012;9(71):1325-1338.
15. Wang W, Tang D, Mao B, et al. A fast-fractional flow reserve simulation method in a patient with coronary stenosis based on resistance boundary conditions. *Comput Model Eng Sci*. 2018;116(2):163-173.
16. Vassilevski YV, Danilov AA, Simakov SS, et al. Patient-specific anatomical models in human physiology. *Russ J Numer Anal Math Model*. 2015;30(3):185-201.
17. Garcia D, Camici PG, Durand LG, et al. Impairment of coronary flow reserve in aortic stenosis. *J Appl Physiol (1985)*. 2009;106(1):113-121.
18. Ge X, Yin Z, Fan Y, Vassilevski Y, Liang F. A multi-scale model of the coronary circulation applied to investigate transmural myocardial flow. *Int J Numer Method Biomed Eng*. 2018;34(10):e3123.
19. Camici PG, d'Amati G, Rimoldi O. Coronary microvascular dysfunction: Mechanisms and functional assessment. *Nat Rev Cardiol*. 2015;12(1):48-62.
20. Liang F, Takagi S, Himeno R, Liu H. Multi-scale modeling of the human cardiovascular system with applications to aortic valvular and arterial stenoses. *Med Biol Eng Comput*. 2009;47(7):743-755.
21. Nitenberg A, Foulst JM, Antony I, Blanchet F, Rahali M. Coronary flow and resistance reserve in patients with chronic aortic regurgitation, angina pectoris and normal coronary arteries. *J Am Coll Cardiol*. 1988;11(3):478-486.
22. Griffith BE. Immersed boundary model of aortic heart valve dynamics with physiological driving and loading conditions. *Int J Numer Method Biomed Eng*. 2012;28(3):317-345.

23. Marom G, Haj-Ali R, Raanani E, Schäfers HJ, Rosenfeld M. A fluid–structure interaction model of the aortic valve with coaptation and compliant aortic root. *Med Biol Eng Comput.* 2012;50(2):173-182.
24. Mynard JP, Davidson MR, Penny DJ, Smolich JJ. A simple, versatile valve model for use in lumped parameter and one-dimensional cardiovascular models. *Int J Numer Method Biomed Eng.* 2012;28(6-7):626-641.
25. Korakianitis T, Shi Y. Numerical simulation of cardiovascular dynamics with healthy and diseased heart valves. *J Biomech.* 2006;39(11):1964-1982.
26. Liang F, Senzaki H, Kurishima C, Sugimoto K, Inuzuka R, Liu H. Hemodynamic performance of the Fontan circulation compared with a normal biventricular circulation: A computational model study. *Am J Physiol Heart Circ Physiol.* 2014;307(7):H1056-H1072.
27. Bonow RO, Carabello BA, Chatterjee K, et al. ACC/AHA 2006 guidelines for the management of patients with valvular heart disease: A report of the American College of Cardiology/American Heart Association Task Force on Practice Guidelines (writing Committee to Revise the 1998 guidelines for the management of patients with valvular heart disease) developed in collaboration with the Society of Cardiovascular Anesthesiologists endorsed by the Society for Cardiovascular Angiography and Interventions and the Society of Thoracic Surgeons. *J Am Coll Cardiol.* 2006;48(3):e1-e148.
28. Liang F, Sugimoto K, Matsuo K, Liu H, Takagi S. Patient-specific assessment of cardiovascular function by combination of clinical data and computational model with applications to patients undergoing Fontan operation. *Int J Numer Method Biomed Eng.* 2015;30(10):1000-1018.
29. Wilson RF, Wyche K, Christensen BV, Zimmer S, Laxson DD. Effects of adenosine on human coronary arterial circulation. *Circulation.* 1990;82(5):1595-1606.
30. Suga H. Ventricular energetics. *Physiol Rev.* 1990;70(2):247-277.
31. Trenouth RS, Phelps NC, Neill WA. Determinants of left ventricular hypertrophy and oxygen supply in chronic aortic valve disease. *Circulation.* 1976;53(4):644-650.
32. Laskey WK, Kussmaul WG 3rd, Noordergraaf A. Systemic arterial response to exercise in patients with aortic valve stenosis. *Circulation.* 2009;119(7):996-1004.
33. Goodwill AG, Dick GM, Kiel AM, Tune JD. Regulation of coronary blood flow. *Compr Physiol.* 2017;7(2):321-382.
34. Meimoun P, Germain AL, Elmekies F, et al. Factors associated with noninvasive coronary flow reserve in severe aortic stenosis. *J Am Soc Echocardiogr.* 2012;25(8):835-841.
35. Eberli FR, Ritter M, Schwitler J, et al. Coronary reserve in patients with aortic valve disease before and after successful aortic valve replacement. *Eur Heart J.* 1991;12(2):127-138.
36. Suga H. Cardiac energetics: From E (max) to pressure-volume area. *Clin Exp Pharmacol Physiol.* 2003;30(8):580-585.
37. Suga H, Yasumura Y, Nozawa T, Futaki S, Igarashi Y, Goto Y. Prospective prediction of O<sub>2</sub> consumption from pressure-volume area in dog hearts. *Am J Physiol.* 1987;252(6 Pt 2):H1258-H1264.
38. Suga H, Hayashi T, Shirahata M. Ventricular systolic pressure-volume area as predictor of cardiac oxygen consumption. *Am J Physiol.* 1981;240(1):H39-H44.
39. Kal JE, Van Wezel HB, Vergroesen I. A critical appraisal of the rate pressure product as index of myocardial oxygen consumption for the study of metabolic coronary flow regulation. *Int J Cardiol.* 1999;71(2):141-148.
40. Lombardo TA, Rose L, Taeschler M, Tuluy S, Bing RJ. The effect of exercise on coronary blood flow, myocardial oxygen consumption and cardiac efficiency in man. *Circulation.* 1953;7(1):71-78.
41. Fujiwara T, Nogami A, Masaki H, et al. Coronary flow characteristics of left coronary artery in aortic regurgitation before and after aortic valve replacement. *Ann Thorac Surg.* 1988;46(1):79-84.
42. Hongo M, Goto T, Watanabe N, et al. Relation of phasic coronary flow velocity profile to clinical and hemodynamic characteristics of patients with aortic valve disease. *Circulation.* 1993;88(3):953-960.
43. Koo B-K. What is the clinical relevance of the discordance between fractional flow reserve and coronary flow reserve? *JACC Cardiovasc Interv.* 2017;10(10):1008-1010.
44. de Bruyne B, Bartunek J, Sys SU, Pijls NH, Heyndrickx GR, Wijns W. Simultaneous coronary pressure and flow velocity measurements in humans: Feasibility, reproducibility, and hemodynamic dependence of coronary flow velocity reserve, hyperemic flow versus pressure slope index, and fractional flow reserve. *Circulation.* 1996;94(8):1842-1849.
45. Tsalalou EP, Anastasiou-Nana M, Agapitos E, et al. Depressed coronary flow reserve is associated with decreased myocardial capillary density in patients with heart failure due to idiopathic dilated cardiomyopathy. *J Am Coll Cardiol.* 2008;52(17):1391-1398.
46. Rigo F, Gherardi S, Galderisi M, et al. The prognostic impact of coronary flow-reserve assessed by Doppler echocardiography in non-ischaemic dilated cardiomyopathy. *Eur Heart J.* 2006;27(11):1319-1323.
47. Singh JP, Evans JC, Levy D, et al. Prevalence and clinical determinants of mitral, tricuspid, and aortic regurgitation (the Framingham Heart Study). *Am J Cardiol.* 1999;83(6):897-902.
48. van de Hoef TP, van Lavieren MA, Damman P, et al. Physiological basis and long-term clinical outcome of discordance between fractional flow reserve and coronary flow velocity reserve in coronary stenoses of intermediate severity. *Circ Cardiovasc Interv.* 2014;7(3):301-311.

49. Kang DY, Ahn JM, Kim YW, et al. Impact of coronary lesion geometry on fractional flow reserve: Data from interventional cardiology research in-cooperation society-fractional flow reserve and intravascular ultrasound registry. *Circ Cardiovasc Imaging*. 2018;11(6): e007087.
50. Toth G, Hamilos M, Pyxaras S, et al. Evolving concepts of angiogram: Fractional flow reserve discordances in 4000 coronary stenoses. *Eur Heart J*. 2014;35(40):2831-2838.

**How to cite this article:** Ge X, Liu Y, Tu S, Simakov S, Vassilevski Y, Liang F. Model-based analysis of the sensitivities and diagnostic implications of FFR and CFR under various pathological conditions. *Int J Numer Meth Biomed Engng*. 2019;e3257. <https://doi.org/10.1002/cnm.3257>